

# Photometric Study of Kepler Asteroseismic Targets

by

J. Molenda-Żakowicz<sup>1</sup>, M. Jerzykiewicz<sup>1</sup> and A. Frasca<sup>2</sup>

<sup>1</sup> Astronomical Institute, University of Wrocław, Kopernika 11,  
51-622 Wrocław, Poland, e-mail: (molenda,mjrz)@astro.uni.wroc.pl

<sup>2</sup> Catania Astrophysical Observatory, Via S.Sofia 78,  
95123 Catania, Italy, e-mail: afr@oact.inaf.it

*Received ...*

## ABSTRACT

Reported are  $UBV$  and  $wby\beta$  observations of 15 candidates for Kepler primary asteroseismic targets and 14 other stars in the Kepler field, carried out at the *M.G. Fracastoro* station of the Catania Astrophysical Observatory. These data serve to plot the 29 stars in two-parameter diagrams with the photometric indices (such as  $B - V$  or  $\delta m_1$ ) and the atmospheric parameters (such as the MK type or  $[\text{Fe}/\text{H}]$ ) as coordinates. The two-parameter diagrams show no evidence of interstellar reddening. The photometric indices  $B - V$  and  $\beta$  are then used to derive photometric effective temperatures,  $T_{\text{eff}}(B - V)$  and  $T_{\text{eff}}(\beta)$ . For  $T_{\text{eff}}(B - V) > 6400$  K, the photometric effective temperatures turn out to be systematically higher than spectroscopic effective temperatures by  $311 \pm 34$  K and  $346 \pm 91$  K for  $T_{\text{eff}}(B - V)$  and  $T_{\text{eff}}(\beta)$ , respectively. For  $T_{\text{eff}}(B - V) < 6250$  K, the agreement between  $T_{\text{eff}}(B - V)$  and the spectroscopic effective temperatures is very good. The photometric surface gravities, derived from  $c_1$  and  $\beta$ , show a range of about a factor of two greater than their spectroscopic counterparts do.

**Key words:** *Stars: photometry – Stars: astrophysical parameters – Stars: interstellar reddening – Space missions: Kepler*

## 1. Introduction

This is a sequel to the spectroscopic study of Kepler<sup>1</sup> asteroseismic targets published by Molenda-Żakowicz et al. (2007, henceforth Paper I). In Paper I, we reported observations of 15 candidates for Kepler primary asteroseismic targets (PATS) and 14 other stars in the Kepler field, carried out at three observatories. For all these stars, we derived the radial velocities, effective temperatures, surface gravities, metallicities, and the projected rotational velocities from two separate sets of data by means of two independent methods. In addition, we estimated the MK type from one of these sets of data.

In Paper I, three stars, HIP 94335, HIP 94734, and HIP 94743, were found to have variable radial-velocity. For HIP 94335 = FL Lyr, a well-known Algol-type eclipsing variable and a double-lined spectroscopic binary, the orbital elements computed from the new data agreed closely with those of Popper et al. (1986). For HIP 94734 and HIP 94743 = V 2077 Cyg, discovered to be single-lined systems, orbital elements were derived for the first time. In addition, HIP 94743 was demonstrated to be a detached eclipsing binary.

In the present paper, the 15 PATS and 14 other stars in the Kepler field will be referred to collectively as the program stars. In Sect. 2, we give an account of our  $UBV$  and  $wby\beta$  photoelectric photometry of these stars. In Sect. 3 we examine

---

<sup>1</sup><http://kepler.nasa.gov/>

the distribution of the program stars in several two-parameter planes. In Sect. 3.1, we plot the program stars in the spectral type,  $B - V$  plane using MK types from Paper I. The  $UBV$  two-color diagram is presented in Sect. 3.2. We use both these diagrams to discuss the interstellar reddening of the program stars. The reddening is further investigated in Sect. 3.3 by means of comparing the  $UBV$  ultraviolet excess with the metallicity parameter  $[\text{Fe}/\text{H}]$  from Paper I. In paying so much attention to the reddening of these not-so-distant stars we have been motivated by the fact that the Kepler Input Catalog, KIC-10, gives  $E(B - V)$  as high as 0.06 mag for some of our program stars. Sect. 3.4 and 3.5 are limited to program stars having spectral type G2 or earlier; in Sect. 3.4 we consider the  $\beta$ ,  $b - y$  diagram, and in Sect. 3.5 we examine correlations of the Crawford's metal-abundance parameters  $\delta m_1(\beta)$  and  $\delta m_1(b - y)$  with  $[\text{Fe}/\text{H}]$ . In Sect. 4 we derive effective temperatures of the program stars from their color indices and compare them with the spectroscopic effective temperatures from Paper I. Sect. 5 is again limited to program stars having spectral type G2 or earlier; for these stars we determine the surface gravities from the  $uvby\beta$  indices and confront them with the spectroscopic values from Paper I. A summary is provided in Sect. 6. Details of the photometric reductions are given in the Appendix.

## 2. Observations and Results

The observations were obtained by JM-Ż at the *M.G. Fracastoro* station (Serra La Nave, Mount Etna, elevation 1750 m) of the Catania Astrophysical Observatory on nine consecutive nights, from 2006 June 23 to July 1, with a photon-counting single-channel photometer, mounted in the Cassegrain focus of a 91-cm telescope. The photometer housed an EMI 9893QA/350 photomultiplier tube, cooled to  $-15^\circ$  C. Johnson  $UBV$  filters were used on four nights, from June 23 to 25, and on July 1. On six nights, from June 25 to 30, the observations were taken with Strömngren  $uvby$  filters; on four nights, June 25 to 28,  $H\beta$  filters were also used. The  $\beta$  photometry was not obtained for stars having spectral types later than G2. The raw magnitudes and color indices of the program stars were corrected for the effects of atmospheric extinction and transformed to the standard systems using standard stars, observed on the same nights as the program stars. Details of the photometric reductions are given in the Appendix.

The results of the  $UBV$  and  $uvby\beta$  photometry are given in Tables 1 and 2, respectively. The values listed are straight means of the magnitudes and the color indices obtained from individual observations. In Table 1, the number of observations,  $N$ , is greater for the magnitudes than for the color indices because the magnitudes were derived not only from observations with filter  $V$ , but also from observations with filter  $y$ . In case of the eclipsing binary HIP 94335 = FL Lyr, the means were computed from observations outside eclipses. This resulted in reducing the number of individual  $B - V$  and  $U - B$  color-indices of HIP 94335 to two. In case of HIP 94743 = V2077 Cyg, all  $UBV$  and  $uvby\beta$  observations were obtained outside eclipses. However, we rejected two discrepant  $UBV$  observations. This decreased the number of individual  $V$  magnitudes to 12, and the number of individual  $B - V$  and  $U - B$  color-indices to two. The standard errors (s.e.) of the color indices of HIP 94335 and HIP 94743 given in Table 1 are the medians of the standard errors of the remaining stars' color-indices.

For the three binaries (the two mentioned in the preceding paragraph, and HIP 94734) the combined magnitudes and color indices given in Tables 1 and 2 need duplicity corrections which will make the magnitudes and color indices pertain to the brighter components. We shall derive the duplicity corrections presently,

T a b l e 1  
UBV photometry of PATS and the remaining program stars

HIP	$V$	s.e.	N	$B - V$	s.e.	$U - B$	s.e.	N
PATS								
93011	9.641	0.008	10	0.401	0.004	-0.047	0.011	4
94335	9.316	0.004	20	0.554	0.004	0.003	0.008	2
94497	9.921	0.006	18	0.933	0.003	0.673	0.004	8
94565	9.351	0.004	10	0.527	0.004	0.058	0.007	4
94734	9.489	0.007	16	0.641	0.004	0.135	0.008	4
95098	9.501	0.005	12	0.537	0.004	-0.003	0.003	6
95637	9.182	0.006	12	0.373	0.003	-0.088	0.004	6
95733	11.022	0.009	26	0.752	0.005	0.185	0.005	10
96634	9.152	0.010	12	0.807	0.004	0.398	0.010	4
96735	9.200	0.015	12	0.871	0.004	0.526	0.014	4
97219	9.028	0.021	10	0.829	0.004	0.468	0.012	4
97337	11.041	0.007	34	1.259	0.004	1.078	0.013	18
97657	9.531	0.004	14	1.066	0.005	0.966	0.013	8
97974	10.017	0.010	14	0.625	0.004	-0.003	0.009	6
98655	10.495	0.008	14	0.767	0.005	0.332	0.007	6
The remaining program stars								
91128	9.909	0.005	30	1.396	0.005	1.185	0.012	14
92922	9.183	0.006	12	0.769	0.004	0.345	0.007	6
94145	8.992	0.007	8	0.242	0.002	0.022	0.017	4
94704	11.168	0.006	28	0.654	0.002	-0.095	0.006	8
94743	9.142	0.012	12	0.335	0.004	-0.035	0.008	4
94898	9.499	0.008	16	0.792	0.002	0.407	0.005	4
95631	9.132	0.010	12	0.779	0.004	0.379	0.006	4
95638	10.581	0.010	34	0.697	0.003	0.182	0.012	8
95843	9.260	0.009	8	0.418	0.002	-0.093	0.008	4
96146	9.089	0.011	8	0.467	0.005	-0.006	0.016	4
97168	10.411	0.007	16	0.618	0.004	0.012	0.009	6
98381	9.916	0.006	18	1.081	0.004	0.998	0.008	8
98829	9.698	0.006	10	0.712	0.006	0.099	0.015	6
99267	10.140	0.010	22	0.468	0.004	-0.312	0.012	6

assuming these stars to be unreddened.

According to Popper et al. (1986), the visual absolute magnitudes,  $M_V$ , of the components of HIP 94335 = FL Lyr are equal to 3.84 and 5.30 mag. Using the  $M_V$  difference, the MK type of F8 V of the primary (see Paper I), and taking into account the fact that the secondary is a main-sequence star (see its  $\log g$  in table XVII of Popper et al. 1986), we get G8 V for the MK type of the secondary from the data tabulated by Lang (1992). The same result was obtained by Popper et al. (1986) from the  $V - R$  color-index. Using these MK types, the observed magnitude and color indices from Table 1, and the tables of intrinsic color-indices (Lang 1992), we derived the duplicity corrections for  $V$ ,  $B - V$ , and  $U - B$  (to be added to the quantity in question). They are listed in Table 3.

For the remaining two stars, which are SB1 systems, the magnitude differences between components are not known. We have estimated the magnitude differences from the systems' mass functions (see Paper I) as follows. We begun with reading

T a b l e 2  
Four-color and  $\beta$  photometry of PATS and the remaining program stars

HIP	$b - y$	s.e.	$m_1$	s.e.	$c_1$	s.e.	$\beta$	s.e.	N
PATS									
93011	0.258	0.009	0.178	0.013	0.520	0.010	2.690	0.010	6
94335	0.365	0.004	0.169	0.006	0.361	0.007	2.623	0.005	18
94497	0.567	0.011	0.403	0.014	0.271	0.020	–	–	10
94565	0.345	0.006	0.163	0.013	0.455	0.017	2.639	0.009	6
94734	0.423	0.007	0.167	0.008	0.407	0.008	2.608	0.007	12
95098	0.330	0.009	0.186	0.014	0.412	0.020	2.617	0.009	6
95637	0.244	0.007	0.164	0.009	0.512	0.006	2.702	0.004	6
95733	0.461	0.008	0.253	0.012	0.248	0.013	–	–	16
96634	0.506	0.007	0.278	0.010	0.344	0.009	–	–	8
96735	0.545	0.004	0.340	0.008	0.310	0.008	–	–	8
97219	0.502	0.022	0.306	0.015	0.365	0.013	–	–	6
97337	0.777	0.014	0.649	0.021	0.131	0.030	–	–	16
97657	0.646	0.007	0.535	0.010	0.241	0.012	–	–	6
97974	0.423	0.008	0.168	0.013	0.295	0.008	2.589	0.008	8
98655	0.473	0.013	0.284	0.018	0.293	0.011	–	–	8
The remaining program stars									
91128	0.894	0.009	0.528	0.015	0.171	0.020	–	–	16
92922	0.527	0.009	0.182	0.014	0.451	0.015	–	–	6
94145	0.127	0.012	0.197	0.017	0.808	0.013	2.808	0.009	4
94704	0.420	0.007	0.186	0.010	0.106	0.015	–	–	20
94743	0.193	0.006	0.183	0.009	0.639	0.010	2.740	0.006	10
94898	0.514	0.007	0.236	0.010	0.395	0.007	–	–	12
95631	0.508	0.004	0.226	0.006	0.406	0.013	–	–	8
95638	0.442	0.009	0.205	0.010	0.344	0.015	–	–	26
95843	0.285	0.008	0.159	0.006	0.447	0.008	2.629	0.007	4
96146	0.323	0.006	0.156	0.013	0.479	0.018	2.663	0.009	4
97168	0.400	0.010	0.195	0.017	0.255	0.023	2.566	0.006	10
98381	0.643	0.008	0.561	0.016	0.234	0.012	–	–	10
98829	0.444	0.004	0.249	0.010	0.196	0.011	–	–	4
99267	0.372	0.007	0.077	0.009	0.166	0.013	2.580	0.008	16

the mass of the primary from the MK type – mass relation (Lang 1992). Next, for an assumed value of the orbital inclination,  $i$ , the mass function yielded the mass of the secondary. Using the same MK type – mass relation as before and assuming the secondary to be a main-sequence star we obtained the secondary’s spectral type. Then, the MK types of the components were transformed to  $M_V$  by means of the MK type –  $M_V$  relation from Lang (1992). Finally, the duplicity corrections were obtained in the same way as for HIP 94335 = FL Lyr.

In case of HIP 94743 = V2077 Cyg we assumed  $i > 70^\circ$  because for smaller  $i$  the eclipses would be rather unlikely to occur in this widely detached system. For  $70^\circ < i < 90^\circ$ , we obtained G7 V for the MK type of the secondary, 1.76 mag for the  $V$  magnitude difference between components, and the  $UBV$  duplicity corrections listed in Table 3.

The last star, HIP 94734, is not known to be eclipsing. Thus, the inclination of the orbit is unknown. We assumed  $\sin i$  to be equal to  $\pi/4$ , the most probable value

T a b l e 3  
Duplicity corrections (in mag)

for	HIP 94335	HIP 94734	HIP 94743
$V$	0.254	0.049	0.198
$B - V$	-0.042	-0.022	-0.053
$U - B$	-0.044	-0.015	-0.029
$b - y$	-0.031	-0.018	-0.040
$m_1$	0.002	0.006	0.013
$c_1$	-0.005	0.003	0.008
$\beta$	0.018	0.003	0.028

for a random distribution of the orbital inclinations. This yielded K7V for the MK type of the secondary, the  $V$  magnitude difference equal to 3.40 mag, and the  $UBV$  duplicity corrections listed in Table 3.

For the  $uvby\beta$  indices, we obtained the duplicity corrections using the above-derived magnitude differences between components; for  $\beta$  we also used the unreddened relation between this index and  $b - y$  from Crawford (1975a) and Olsen (1988) to estimate the  $\beta$  indices of the secondaries. The duplicity corrections are given in Table 3.

### 3. Two-Parameter Diagrams

#### *3.1. The $B - V$ color-indices and the MK types*

In Fig. 1, the  $B - V$  color-indices from Table 1 are plotted vs. the spectral type from Table 9 of Paper I. In case of the binaries, HIP 94335, HIP 94734 and HIP 94743, we applied the duplicity corrections to  $B - V$  (see the preceding section). The solid line represents the intrinsic relation for luminosity class (LC) V, and the dashed line, for LC III (Lang 1992). The distances,  $r$  (in parsecs) used in coding the symbols, were obtained from the Hipparcos parallaxes (ESA 1997) revised by van Leeuwen (2007). The symbols joined with dotted lines are the two subdwarfs (open diamonds) and the two LC III stars (open circles). The remaining program stars were classified in Paper I to LC V, IV-V, IV or IV-III.

As can be seen from Fig. 1, most program stars lie within less than one spectral subtype of the intrinsic relations. Five deviate by two subtypes. Three deviate by more than two subtypes. The latter are the two subdwarfs (the open diamonds joined with dotted line) and HIP 94743, the small filled circle at  $B - V \approx 0.28$  mag. Both subdwarfs deviate from the intrinsic relation for LC V by about four subtypes in the direction of earlier types. Qualitatively, this may be understood as an abundance effect: in F and G stars the lines of neutral metals strengthen with advancing type, so that smaller metallicity may mimic earlier type. In case of HIP 94743 = V2077 Cyg, the color index indicates a spectral type of about A9, some three subtypes earlier than F2, assigned to it in Paper I. This discrepancy would disappear if the color index were *redder* by 0.07 mag, but an error of this magnitude in the  $B - V$  seems rather unlikely. This is supported by the fact that the star's  $uvby\beta$  indices also indicate earlier spectral type (see Sect. 3.4).

In  $B - V$ , the points in Fig. 1 seem to scatter randomly around the LC V intrinsic relation. (Note that the two LC III program stars fall in the lower left-hand corner

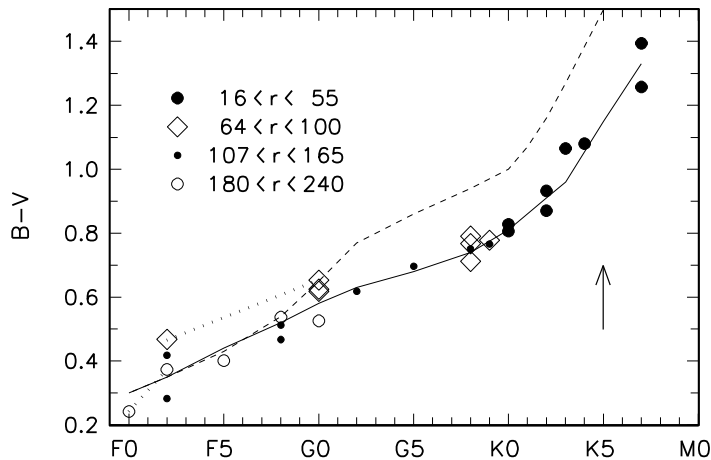


Figure 1: The  $B - V$  color-indices of the program stars plotted as a function of the spectral type. The solid line represents the intrinsic relation for luminosity class V, and the dashed line, for luminosity class III (Lang 1992). The distances,  $r$  (in parsecs) used in coding the symbols, were obtained from the revised Hipparcos parallaxes (van Leeuwen 2007). The symbols joined with dotted lines are the two subdwarfs (open diamonds) and the two luminosity III stars (the leftmost open circles). The arrow is the reddening vector  $E(B - V) = 0.2$  mag.

of the figure where the LC V and LC III lines coincide.) In order to quantify this impression, we computed the deviations in  $B - V$  from the intrinsic relations,  $(B - V) - (B - V)_0$ . For LC V and LC III we read  $(B - V)_0$  from the Lang's (1992) relations shown in the figure. For LC IV we used intrinsic values half-way between LC V and LC III, for LC IV-V, the values half-way between LC V and LC IV, and for LC III-IV, those half-way between LC IV and LC III. The mean deviation (omitting the two subdwarfs) turned out to be equal to  $-0.009 \pm 0.010$  mag. In the intervals of distance indicated in the figure, the mean deviations amounted to  $0.016 \pm 0.020$  mag for  $16 < r < 55$  pc,  $-0.026 \pm 0.023$  mag for  $64 < r < 100$  pc,  $-0.007 \pm 0.015$  mag for  $107 < r < 165$  pc, and  $-0.031 \pm 0.020$  mag for  $180 < r < 240$  pc.

Note that de-reddening makes the  $(B - V) - (B - V)_0$  deviations decrease. Therefore, de-reddening will make the overall agreement with the intrinsic relations worse than that seen in the figure, except for an unlikely case of  $E(B - V) \leq 0.030$  mag for  $r < 55$  pc and  $E(B - V) = 0$  mag for  $r > 64$  pc. We conclude that there is no evidence in Fig. 1 for  $E(B - V) > 0.00$  mag even for the most distant stars in our sample.

### 3.2. The $UBV$ Two-Color Diagram

Fig. 2 shows the program stars plotted in the two-color diagram using the  $B - V$  and  $U - B$  color-indices from Table 1. In case of the binaries, HIP 94335, HIP 94734 and HIP 94743, we applied the duplicity corrections derived in Sect. 2. The distances,  $r$  (in parsecs) used in coding the symbols, were obtained from the revised Hipparcos parallaxes (van Leeuwen 2007). In the figure there is also plotted the Hyades main-sequence two-color line, explained in the next paragraph, and the Hyades line reddened with  $E(B - V) = 0.05$  mag and  $E(U - B) = 0.72E(B - V)$ .

The two frequently used Hyades two-color relations are (1) that given by Sandage & Eggen (1959) in their Table III, and (2) Johnson's (1966) main-sequence relation,

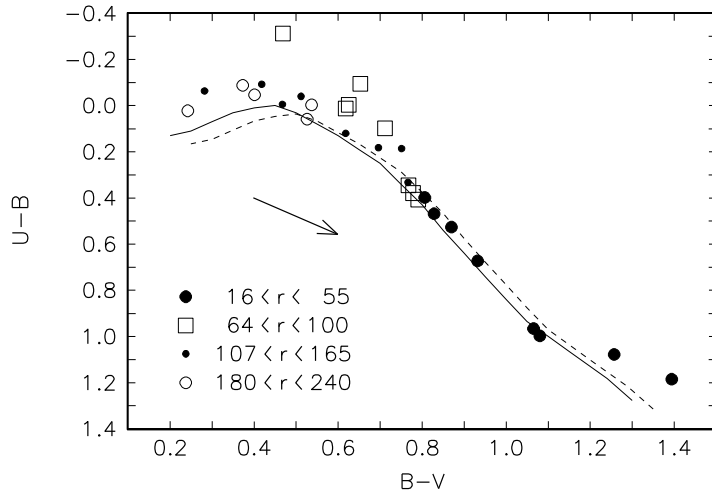


Figure 2: Program stars in the two-color plane. The distances,  $r$  (in parsecs) used in coding the symbols, were obtained from the revised Hipparcos parallaxes (van Leeuwen 2007). The solid line represents the Hyades two-color relation. The arrow is the reddening vector  $E(B - V) = 0.2$  mag and  $E(U - B) = 0.72E(B - V)$ . The dashed line is the Hyades relation reddened with  $E(B - V) = 0.05$  mag.

listed in his Table II (used in lieu of the Hyades line by, e.g., Cameron 1985). The two lines agree closely for  $0.20 < B - V < 0.95$  mag. For  $B - V > 0.95$  mag, Johnson’s (1966) line veers upwards. In order to decide which line is the more nearly correct one, we have used the list of the Hyades’ members composed by Pinsonneault et al. (2004) and  $UBV$  color-indices determined by Johnson and Knuckles (1955) and Mendoza (1967). Plotted in the  $B - V$ ,  $U - B$  plane, these data resulted in a point-diagram. A free-hand curve drawn through the points coincided with the two-color relation of Sandage and Eggen (1959). The solid line in Fig. 2 is this relation, slightly smoothed on the red side of  $B - V = 1.00$  mag and extended to  $B - V = 1.30$  mag, 0.20 mag beyond the last  $B - V$  value of Sandage & Eggen (1959). For  $1.05 < B - V < 1.30$  mag, Johnson’s (1966) main-sequence relation – not shown in the figure to avoid crowding – would coincide with our  $E(B - V) = 0.05$  mag line.

In Fig. 2, most stars with  $B - V < 0.76$  mag show ultraviolet excess. This will be discussed in the next subsection. Stars with  $0.76 < B - V < 1.10$  mag lie on or very close to the Hyades line. Assuming zero reddening for the Hyades (Crawford 1975a, Taylor 1980), we conclude that these stars are unreddened.

HIP 97337 and HIP 91128, the two red stars having  $B - V > 1.25$  mag (both classified to K7V in Paper I), deviate from the Hyades line. If the deviations were caused by reddening, the  $E(B - V)$  would have to be equal to 0.21 mag for HIP 97337 and 0.34 mag for HIP 91128. Neither value agrees with the stars’  $(B - V) - (B - V)_0$  deviations in Fig. 1 and, of course, with the fact that they are among the least distant stars in our sample ( $37 \pm 2$  and  $15.5 \pm 0.2$  pc, respectively).

### 3.3. The Ultraviolet Excess and $[\text{Fe}/\text{H}]$

The ultraviolet excess,  $\delta(U - B)$ , is defined as the difference between the Hyades  $U - B$  at the star’s  $B - V$  and the star’s  $U - B$ . It is a function of the star’s LC, metallicity, reddening and rotation. For the stars plotted in Fig. 2, the last factor

will be neglected. Some justification for this comes from the fact that 22 stars in our sample have  $v \sin i < 10 \text{ km s}^{-1}$ , and the remaining ones have  $20 < v \sin i < 35 \text{ km s}^{-1}$  (see Table 12 of Paper I). The first factor can be corrected for using the MK luminosity classification of Paper I and the intrinsic UBV color-indices for the LCs V and III tabulated by Lang (1992). The correction, to be subtracted from  $\delta(U - B)$ , amounts to the difference between the tabular  $U - B$  at the star's  $B - V$  and LC and the tabular  $U - B$  at the same  $B - V$  and LC V. For LC IV, we assumed the corrections to be equal to one-half of those for LC III. Likewise, the corrections for the LCs IV-V and III-IV were assumed to be equal to one-quarter and three-quarters of those for LC III, respectively. The corrections ranged from 0.010 mag for HIP 94898 (G8 IV) to 0.078 mag for HIP 95637 (F2 III).

The  $\delta(U - B)$  values, corrected in this way for the program stars of luminosity classes IV-V, IV, III-IV, and III, are listed in the third column of Table 4. These values are functions of metallicity and  $B - V$ , so that stars with the same metal abundance but different  $B - V$  will have different  $\delta(U - B)$ . In the fourth column of Table 4 there are given the  $\delta$  correction factors,  $\delta 0.6/\delta$ , which can be used to transform the observed  $\delta(U - B)$  into  $\delta(0.6)$ , a measure of metallicity independent of  $B - V$ . We computed these factors from the  $\delta = f(B - V)$  relation given by Sandage (1969) in his Table 1A. In case of two program stars that have  $B - V < 0.35$  mag, HIP 94145 and HIP 94743, we had to extrapolate the  $\delta = f(B - V)$  relation beyond  $B - V = 0.35$  mag, the smallest  $B - V$  in Sandage's (1969) Table 1A. Extrapolation was also needed for the subdwarf HIP 99267 because its  $\delta(U - B)$  is larger than the largest  $\delta(U - B)$  in Sandage's (1969) Table 1A. These three  $\delta$  correction factors are less secure than the other ones. For the two red stars, HIP 97337 and HIP 91129, no  $\delta$  correction factors were derived. Note that most  $\delta$  correction factors in Table 4 are equal to 1.000.

In Fig. 3, the metallicity parameter,  $[\text{Fe}/\text{H}]$ , is plotted as a function of  $\delta(0.6)$ . The standard errors of  $\delta(0.6)$  were assumed to be equal to the standard error of the  $U - B$  color-index (see Table 1) times the  $\delta$  correction factor. In both panels, the horizontal solid line indicates  $[\text{Fe}/\text{H}] = 0.13$ , the Hyades' value of the metallicity parameter according to Boesgaard & Friel (1990). The inclined lines represent the  $[\text{Fe}/\text{H}]$ - $\delta(0.6)$  relations for main-sequence stars due to Karataş & Schuster (2006) and Cameron (1985). The lower panel contains all program stars except the two red ones, HIP 97337 and HIP 91128. In the upper panel, which shows the upper left-hand part of the lower panel, there are plotted stars having (1)  $B - V < 0.50$  mag, or (2)  $B - V > 0.70$  mag. As can be seen from Fig. 2, de-reddening group 1 stars would increase their ultraviolet excesses, while the reverse is true for group 2 stars. Thus, de-reddening these stars alters their position in relation to the  $[\text{Fe}/\text{H}]$ - $\delta(0.6)$  lines in Fig. 3. In the next paragraph, we shall use this facts to discuss the reddening. Stars with  $0.50 < B - V < 0.70$  mag are not plotted in the upper panel of Fig. 3 because in this  $B - V$  interval the reddening vector is very nearly parallel to the Hyades line (see Fig. 2), and therefore  $\delta(U - B)$  will not be affected by reddening. Consequently, the position of these points in relation to the  $[\text{Fe}/\text{H}]$ - $\delta(0.6)$  lines in Fig. 3 carries no information about  $E(B - V)$ .

As can be seen from Fig. 3, all group 1 stars (including the subdwarf HIP 99267, not plotted in the upper panel) lie either very close to the  $[\text{Fe}/\text{H}]$ - $\delta(0.6)$  lines (HIP 96146, HIP 93011, HIP 95637, in order of decreasing  $[\text{Fe}/\text{H}]$ ) or on the right-hand side of it (HIP 94145, HIP 95843, HIP 94743, HIP 99267, in order of increasing distance from the  $[\text{Fe}/\text{H}]$ - $\delta(0.6)$  lines). De-reddening the  $B - V$  and  $U - B$  color-indices would move a group 1 star to the right in Fig. 3. As an example, let us consider HIP 96146, the star represented in the upper panel of Fig. 3 by the leftmost open circle lying about half the standard error (equal to 0.016 mag) to the left of the

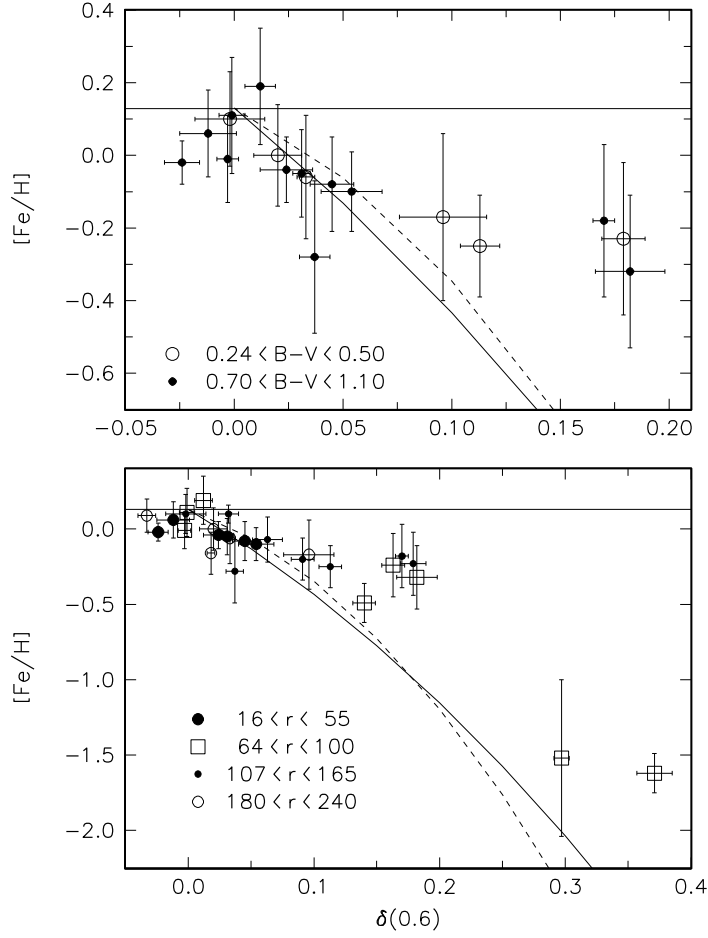


Figure 3: The metallicity parameter  $[Fe/H]$  plotted as a function of  $\delta(0.6)$ . The lower panel contains all program stars except the two red ones, HIP 97337 and HIP 91128. In the upper panel, which shows the upper left-hand part of the lower panel, stars with  $0.50 < B - V < 0.70$  are not plotted. Note that in the lower panel the symbols are coded as in Fig. 2, while in the upper panel the symbols are coded according to the  $B - V$ . The horizontal solid lines indicate  $[Fe/H] = 0.13$ , the Hyades' metallicity parameter according to Boesgaard & Friel (1990). The inclined solid line represents the  $[Fe/H]$ - $\delta(0.6)$  relation for main-sequence stars due to Karataş & Schuster (2006), and the dashed line, that due to Cameron (1985).

T a b l e 4  
The color index, ultraviolet excess,  $\delta$  correction factor, and the metallicity parameter [Fe/H] from Paper I

HIP	$B - V$	$\delta(U - B)$	$\delta 0.6/\delta$	[Fe/H]	s.d.
PATS					
93011	0.401	0.019*	1.035	0.00	0.14
94335	0.512	0.084	1.078	-0.20	0.14
94497	0.932	0.031	1.000	-0.05	0.12
94565	0.526	-0.033*	1.000	0.09	0.11
94734	0.618	0.032	1.000	0.10	0.06
95098	0.537	0.018*	1.000	-0.16	0.14
95637	0.373	0.031*	1.056	-0.06	0.17
95733	0.751	0.157	1.080	-0.18	0.21
96634	0.806	0.045	1.000	-0.08	0.13
96735	0.870	0.054	1.000	-0.10	0.11
97219	0.828	0.024	1.000	-0.04	0.09
97337	1.257	0.131	-	-0.15	0.15
97657	1.065	-0.012	1.000	0.06	0.12
97974	0.625	0.163	1.000	-0.24	0.21
98655	0.766	0.037	1.000	-0.28	0.21
The remaining program stars					
91128	1.394	0.243	-	-0.17	0.15
92922	0.767	0.012*	1.000	0.19	0.16
94145	0.242	0.080*	1.200	-0.17	0.23
94704	0.653	0.289	1.026	-1.52	0.52
94743	0.282	0.148	1.208	-0.23	0.21
94898	0.791	-0.003*	1.000	-0.01	0.12
95631	0.778	-0.001*	1.000	0.11	0.16
95638	0.696	0.063	1.000	-0.07	0.15
95843	0.418	0.097	1.161	-0.25	0.14
96146	0.467	-0.002*	1.000	0.10	0.13
97168	0.618	0.140	1.000	-0.40	0.13
98381	1.080	-0.024	1.000	-0.02	0.06
98829	0.712	0.173	1.053	-0.32	0.21
99267	0.468	0.323	1.150	-1.62	0.13

\* Corrected for the luminosity effect as described in the text.

[Fe/H] $-\delta(0.6)$  lines. If we assumed  $E(B - V) = 0.05$  mag, the  $\delta(0.6)$  would change from  $-0.002$  mag to  $0.033$  mag. The open circle would then move to the right by two standard errors, so that the distance from the [Fe/H] $-\delta(0.6)$  lines would increase to 1.5 standard error. For the remaining group 1 stars, de-reddening would spoil the agreement with the [Fe/H] $-\delta(0.6)$  lines even more. We conclude that for group 1 stars, including the two most distant program stars HIP 93011 ( $r = 242 \pm 42$  pc) and HIP 94145 ( $r = 229 \pm 36$  pc), their position in the  $\delta(0.6)$ , [Fe/H] plane implies  $E(B - V) < 0.025$  mag.

De-reddening a group 2 star moves it to the left in Fig. 3. Thus, de-reddening may move a group 2 star closer to the [Fe/H] $-\delta(0.6)$  lines if it lies on the right-hand side of them. Most such stars lie less than one standard error (of [Fe/H],  $\delta(0.6)$ , or both) off the lines. However, HIP 95733 and HIP 98829, represented by the two rightmost points in the upper panel of Fig. 3, deviate by more than three standard errors from the [Fe/H] $-\delta(0.6)$  lines. Shifting these two points so that they would lie between the two [Fe/H] $-\delta(0.6)$  lines would require  $E(B - V) = 0.14$  mag for HIP 95733 and  $E(B - V) = 0.21$  mag for HIP 98829. De-reddening HIP 95733 and HIP 98829 using these numbers would make their  $B - V$  color-indices much too blue for the stars' MK type, G8 V in both cases (see Table 9 of Paper I). In addition, the two stars lie very close to the Lang's (1992) intrinsic relation in Fig. 1. We conclude that reddening cannot explain the rightward deviation of HIP 95733 and HIP 98829 from the [Fe/H] $-\delta(0.6)$  lines.

In addition to these two stars, and the group 1 star HIP 94743 = V 2077 Cyg (the open circle at  $\delta(0.6) \approx 0.18$  in the upper panel of Fig. 3), the subdwarf, HIP 99267 (the rightmost open square in the lower panel of Fig. 3) also deviates from the mean [Fe/H] $-\delta(0.6)$  relations by several standard errors in the abscissa. These deviations require explaining.

#### 3.4. The $\beta$ , $b - y$ Diagram

In Fig. 4, the program stars for which the  $\beta$  index has been measured by us are plotted in the  $\beta$ ,  $b - y$  plane using the values from Table 2, with the duplicity corrections for HIP 94335, HIP 94734 and HIP 94743 (see Table 3) taken into account. The distances,  $r$  (in parsecs) used in coding the symbols, were obtained from the revised Hipparcos parallaxes (van Leeuwen 2007). The solid line is the standard relation of Crawford (1975a) (with slight corrections due to Olsen 1988), valid for unreddened F0–G2 stars of luminosity classes III–V. The long-dashed line is Crawford's (1979) standard relation for A7–F0 stars. The short-dashed lines represent the envelopes of scatter in Crawford's (1975a) F-star  $\beta$ ,  $b - y$  diagram (his Fig. 1); they show by how much an unreddened F-type star may deviate from the standard relation because of – to use Crawford's term – “cosmic scatter.” The arrow is the reddening vector  $E(b - y) = 0.074$  mag, corresponding to  $E(B - V) = 0.1$  mag (Crawford 1975b).

In Fig. 4, the deviations in the ordinate,  $(b - y) - (b - y)_0$ , where  $(b - y)_0$  is the standard  $b - y$  at the star's  $\beta$ , range from  $-0.066$  mag for HIP 99267, the F2 subdwarf, to  $0.026$  mag for HIP 96146. The mean deviation is equal to  $-0.015 \pm 0.009$  mag. However, HIP 97168 (the rightmost open square in the figure), which shows the negative deviation of  $-0.063$  mag, may do so because of (slight) emission in the H $\beta$  line at the time of observation (see the next subsection). If we rejected HIP 97168 and the subdwarf, the mean deviation would become equal to  $-0.006 \pm 0.008$  mag. For the five stars more distant than 180 pc, the mean deviation amounts to  $-0.008 \pm 0.008$  mag. Since de-reddening would decrease the  $b - y$  deviations, we conclude that there is no evidence for reddening in Fig. 4.

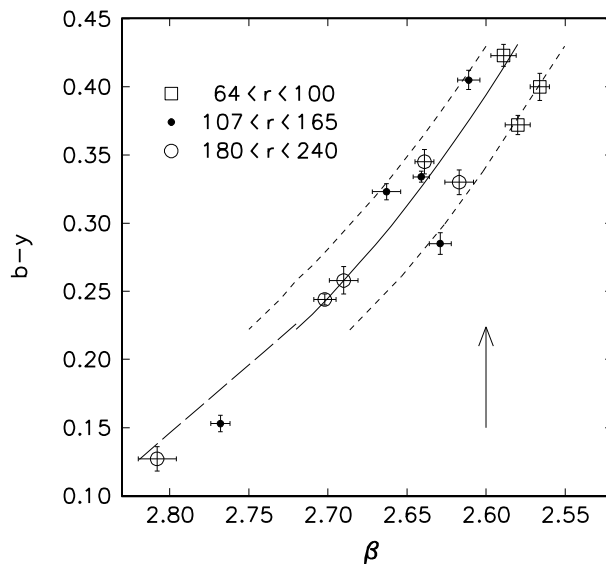


Figure 4: Program stars in the  $\beta$ ,  $b - y$  plane. The distances,  $r$  (in parsecs) used in coding the symbols, were obtained from the revised Hipparcos parallaxes (van Leeuwen 2007). The solid line represents the standard relation of Crawford (1975a) (with slight corrections due to Olsen 1988), valid for unreddened F0–G2 stars of luminosity classes III–V. The long-dashed line is Crawford’s (1979) standard relation for A7–F0 stars. The short-dashed lines show by how much an unreddened F-type star may deviate from the standard relation because of “cosmic scatter” (see Crawford 1975a, Fig. 1). The arrow is the reddening vector  $E(b - y) = 0.074$  mag, corresponding to  $E(B - V) = 0.1$  mag (Crawford 1975b).

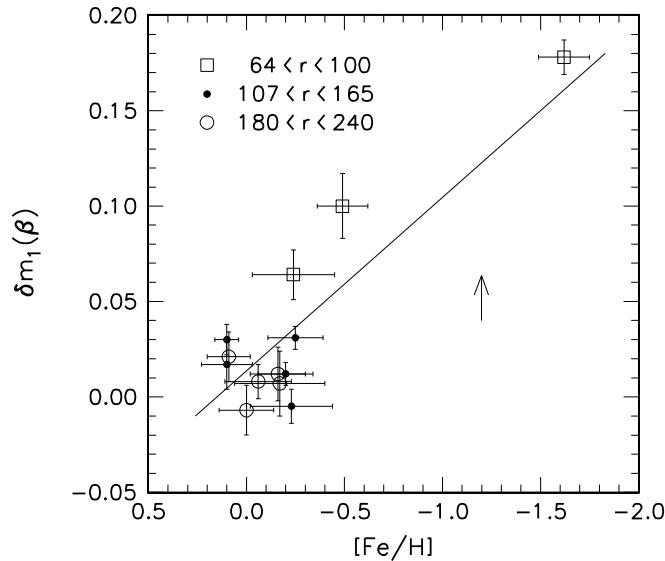


Figure 5: Program stars in the  $[\text{Fe}/\text{H}]$ ,  $\delta m_1(\beta)$  plane. The symbols are coded as in Fig. 4. The line represents the  $[\text{Fe}/\text{H}]$ - $\delta m_1(\beta)$  relation of Crawford & Perry (1976). The arrow is the reddening vector  $E(m_1) = -0.024$  mag, corresponding to  $E(B - V) = 0.1$  mag (Crawford 1975b).

In Sect. 3.1 we noted that HIP 94743, classified to F2 in Paper I, showed a deviation from the intrinsic relation in Fig. 1 which suggested a spectral type of about A9. In Fig. 4, this star (the leftmost filled circle) falls close to Crawford’s (1979) standard relation for A7–F0 stars (the long-dashed line).

### 3.5. The $[\text{Fe}/\text{H}]$ , $\delta m_1$ Diagrams

Crawford (1975a) has defined metal-abundance parameters  $\delta m_1(\beta)$  and  $\delta m_1(b - y)$ . In both cases, the parameter is a difference between the standard and observed value of  $m_1$  (in the sense “standard *minus* observed”); in case of  $\delta m_1(\beta)$ , the standard value is read from the standard relations between the  $uvby\beta$  indices using the observed  $\beta$  as the independent variable; in case of  $\delta m_1(b - y)$ , the independent variable is the observed  $b - y$ , corrected for reddening if necessary.

Figs. 5 and 6 show the program stars in the  $[\text{Fe}/\text{H}]$ ,  $\delta m_1(\beta)$  and the  $[\text{Fe}/\text{H}]$ ,  $\delta m_1(b - y)$  planes using the  $[\text{Fe}/\text{H}]$  values from Table 9 of Paper I and the  $uvby\beta$  indices from Table 2. For HIP 94335, HIP 94734 and HIP 94743 the duplicity corrections (see Table 3) were taken into account. Zero reddening was assumed in drawing both figures. Fig. 6 shows one more program star than Fig. 5 does, viz., HIP 94704, the G0 subdwarf for which  $\beta$  was not measured (the open square with the long horizontal error bar). For most stars, we used the F-star standard  $m_1 - \beta$  and  $m_1 - (b - y)$  relations from Table I of Crawford (1975a); for HIP 97168 (the rightmost open square in Fig. 4) the standard  $m_1 - \beta$  relation had to be extrapolated. For two stars, HIP 94743 and HIP 94145 (the leftmost filled circle and the leftmost open circle in Fig. 4, respectively) we used Crawford’s (1979) A-star standard relation.

In Figs. 5 and 6 all points in common but one show similar deviations from the  $[\text{Fe}/\text{H}]$ - $\delta m_1$  relations of Crawford & Perry (1976). The exception is HIP 97168 (the open square at  $[\text{Fe}/\text{H}] = -0.5$ ) for which  $\delta m_1(\beta) = 0.100$  mag while  $\delta m_1(b - y) =$

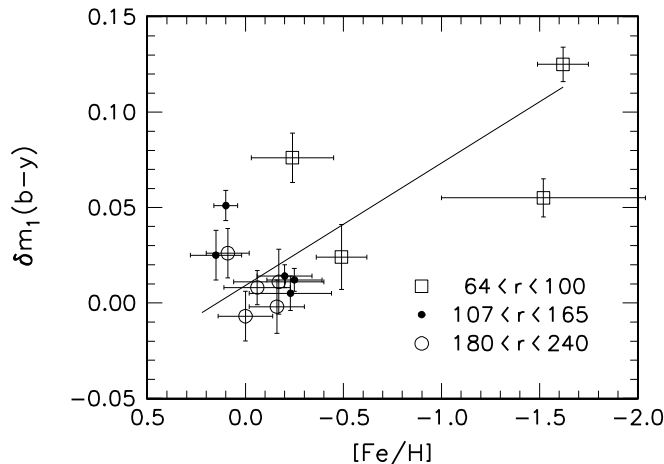


Figure 6: Program stars in the  $[\text{Fe}/\text{H}]$ ,  $\delta m_1(b-y)$  plane. The symbols are coded as in Fig. 4. The line represents the  $[\text{Fe}/\text{H}]$ - $\delta m_1(b-y)$  relation of Crawford & Perry (1976).

0.024 mag. The discrepancy would disappear if the star's  $\beta$  were increased by 0.030 mag. This suggests a slight emission at  $\text{H}\beta$  at the time of observation.

#### 4. The Effective Temperatures

##### 4.1. Photometric Effective Temperatures

For all Population I program stars we can obtain  $T_{\text{eff}}$  from the  $B-V$  color-index. In case of the stars for which we have measured the  $\beta$  index, we can also derive  $T_{\text{eff}}$  from this index. We shall denote these photometric effective temperatures by  $T_{\text{eff}}(B-V)$  and  $T_{\text{eff}}(\beta)$ , respectively. In case of the subdwarfs,  $T_{\text{eff}}$  is also a function of a metallicity parameter (see below).

For deriving  $T_{\text{eff}}(B-V)$ , we used the  $B-V$  color-indices from Table 1 (plus the duplicity corrections in case of the binaries HIP 94335, HIP 94734 and HIP 94743) and Flower's (1996)  $T_{\text{eff}}$  vs.  $(B-V)$  calibration (his Table 3). For  $T_{\text{eff}}(\beta)$ , we used the  $uvby\beta$  indices from Table 2 (with the duplicity corrections in case of the binaries) and the FORTRAN program UVBYBETA<sup>2</sup>, kindly made available to us by Dr. Napiwotzki. In both cases, we assumed the color indices to be unreddened. The results are given in Table 5.

The program UVBYBETA requires all four  $uvby\beta$  indices as input. However, for F and G stars, the effective temperature is derived from the  $\beta$  index, with a marginal contribution from  $c_1$ . Therefore,  $T_{\text{eff}}(\beta)$  was not obtained for HIP 97168 because of the suspected emission at  $\text{H}\beta$  (see Sect. 3.5).

For the two subdwarfs, HIP 94704 and HIP 99267, we computed  $T_{\text{eff}}$  from  $B-V$  and  $\delta(0.6)$  using the calibration of Carney et al. (1994), and from  $b-y$  and  $[\text{Fe}/\text{H}]$  using the calibration of Spite et al. (1996). The color indices were assumed to be unreddened. These effective temperatures we shall refer to as  $T_{\text{eff}}(B-V, \delta(0.6))$  and  $T_{\text{eff}}(b-y, [\text{Fe}/\text{H}])$ , respectively. They are also listed in Table 5.

A comparison of the photometric effective temperatures is shown in Fig. 7,

<sup>2</sup>Written in 1985 by T.T. Moon of the University London and modified in 1992 by R. Napiwotzki of Universitaet Kiel. The program is based on the grid published in Moon & Dworetzky (1985)

T a b l e 5  
The photometric effective temperatures

HIP	$T_{\text{eff}}(B - V)$	s.e.	$T_{\text{eff}}(\beta)$	s.e.
PATS				
93011	6720	18	6810	93
94335	6232	17	6423	55
94497	4980	6	–	–
94565	6175	16	6340	103
94734	5856	14	6029	92
95098	6130	16	6105	116
95637	6853	14	6925	37
95733	5411	14	–	–
96634	5267	10	–	–
96735	5114	9	–	–
97219	5212	10	–	–
97337	4387	7	–	–
97657	4722	9	–	–
97974	5802	14	5810	115
98655	5370	13	–	–
The remaining program stars				
91128	4163	8	–	–
92922	5367	11	–	–
94145	7525	11	7754	82
94704	5182	11	5490	48
94743	7547	133	7449	56
94898	5305	5	–	–
95631	5339	10	–	–
95638	5571	9	–	–
95843	6642	9	6229	85
96146	6422	22	6576	9
97168	5827	14	–	–
98381	4695	7	–	–
98829	5523	17	–	–
99267	5639	28	5748	41

For HIP 94704 and HIP 99267  $T_{\text{eff}}(B - V, \delta(0.6))$  is given instead of  $T_{\text{eff}}(B - V)$ , and  $T_{\text{eff}}(b - y, [\text{Fe}/\text{H}])$ , instead of  $T_{\text{eff}}(\beta)$ .

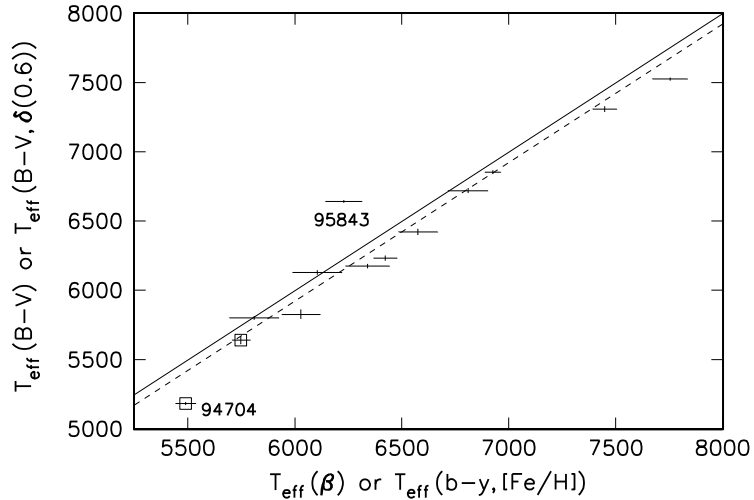


Figure 7: Comparison of the photometric effective temperatures. Population I stars are shown with the crossed error bars, and the subdwarfs, with open squares. The solid line has unit slope and zero intercept. The short-dashed line corresponds to the straight mean difference  $T_{\text{eff}}(B-V) - T_{\text{eff}}(\beta)$ . HIP numbers label points that deviate from the short-dashed line by more than  $3\sigma$ , where  $\sigma$  is the standard deviation of an individual temperature difference (very nearly a half of the corresponding horizontal error bar).

where  $T_{\text{eff}}(B-V)$  is plotted as a function of  $T_{\text{eff}}(\beta)$  for Population I stars, and  $T_{\text{eff}}(B-V, \delta(0.6))$  is plotted as a function of  $T_{\text{eff}}(b-y, [\text{Fe}/\text{H}])$  for the subdwarfs. The straight mean difference  $T_{\text{eff}}(B-V) - T_{\text{eff}}(\beta)$  is equal to  $-74 \pm 54$  K. In the figure, the short-dashed line is shifted by this number from the solid line which has unit slope and zero intercept. The points that deviate from the short-dashed line by more than  $3\sigma$ , where  $\sigma$  is the standard deviation of an individual temperature difference (very nearly a half of the corresponding horizontal error bar) are labeled with the HIP numbers.

#### 4.2. Comparison with Spectroscopic Effective Temperatures

In Paper I, we have derived the spectroscopic effective temperatures of program stars by two methods. In the present discussion we shall call these methods (1) and (2). In method (1), we compared the spectrograms, obtained with the Catania Astrophysical Observatory’s fiber-fed echelle spectrograph FRESKO on a 91-cm telescope, with spectrograms of reference stars with known atmospheric parameters. In addition to  $T_{\text{eff}}$ , this method yielded  $\log g$ ,  $[\text{Fe}/\text{H}]$  and the MK type. We used two independent grids of reference stars. One was based on spectrograms selected from an archive known as ELODIE (Prugniel & Soubiran 2001), and the other, on reference stars observed with FRESKO. We shall refer to the effective temperatures derived with the ELODIE grid as  $T_{\text{eff}}(1\text{E})$ , and those derived with the FRESKO grid, by  $T_{\text{eff}}(1\text{F})$ . In Paper I,  $T_{\text{eff}}(1\text{E})$  and the remaining atmospheric parameters obtained with the ELODIE grid are listed in Table 9, and those obtained with the FRESKO grid, in Table 10. Table 9 contains all program star, while Table 10, only 16, having  $T_{\text{eff}}$  in the range from about 5000 K to about 6000 K. The MK types and the metallicity parameters  $[\text{Fe}/\text{H}]$  already discussed in the present paper have

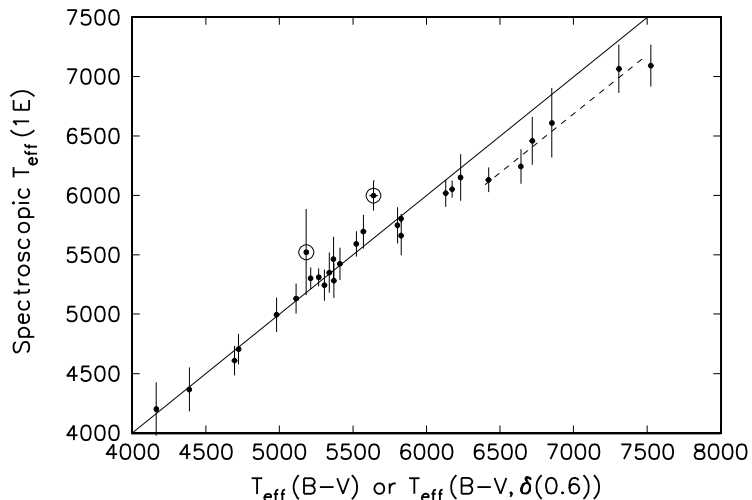


Figure 8: The spectroscopic effective temperature  $T_{\text{eff}}(1E)$  plotted as a function of  $T_{\text{eff}}(B-V)$  for Population I stars (points), and  $T_{\text{eff}}(B-V, \delta(0.6))$  for the subdwarfs (encircled points). HIP 94743 (the rightmost point) was shifted up and to the right to avoid coincidence with HIP 94145. The horizontal error bars are too short to show up. The solid line has unit slope and zero intercept; the short-dashed line runs 311 K below it.

been taken from Table 9.

In method (2), we used echelle spectrograms obtained with the CfA Digital Speedometers at the Oak Ridge Observatory, Harvard, Massachusetts and the F.L. Whipple Observatory, Mount Hopkins, Arizona. From these spectrograms,  $T_{\text{eff}}$  and  $\log g$  were determined by cross-correlation with templates computed from model stellar atmospheres. We shall refer to the effective temperatures derived by this method as  $T_{\text{eff}}(2)$ . In Paper I,  $T_{\text{eff}}(2)$  are listed in Table 11.

The spectroscopic effective temperatures  $T_{\text{eff}}(1E)$  are plotted in Fig. 8 vs.  $T_{\text{eff}}(B-V)$  for Population I stars, and vs.  $T_{\text{eff}}(B-V, \delta(0.6))$  for the subdwarfs. As can be seen from the figure, at  $T_{\text{eff}}(B-V) < 6250$  K the points scatter randomly around the line of unit slope and zero intercept, with only the subdwarfs showing large deviations. For  $T_{\text{eff}}(B-V) < 6250$  K, the mean difference  $T_{\text{eff}}(1E) - T_{\text{eff}}(B-V)$  amounts to an insignificant  $-15 \pm 17$  K. However, for  $T_{\text{eff}}(B-V) > 6400$  K all points fall below the line. For these points, the mean difference  $T_{\text{eff}}(1E) - T_{\text{eff}}(B-V)$  is equal to  $-311 \pm 34$  K; this mean difference was used to draw the short-dashed line in Fig. 8. If  $T_{\text{eff}}(\beta)$  were used instead of  $T_{\text{eff}}(B-V)$ , the mean difference for  $T_{\text{eff}}(B-V) > 6400$  K would be equal to  $-356 \pm 90$  K. Since  $T_{\text{eff}}(\beta)$  and  $T_{\text{eff}}(B-V)$  were obtained independently of each other, the systematic deviation for  $T_{\text{eff}}(B-V) > 6400$  K must be due to a problem in deriving  $T_{\text{eff}}(1E)$  for the six hottest stars in our sample.

The effective temperatures obtained with the FRESKO grid may suffer from the same problem because for the two stars with  $T_{\text{eff}}(B-V) > 6400$  K, HIP 95843 and HIP 96146, for which  $T_{\text{eff}}(1F)$  were derived, the mean difference  $T_{\text{eff}}(1F) - T_{\text{eff}}(B-V)$  is equal to  $-370$  K.

A comparison of the spectroscopic effective temperatures based on model stellar atmospheres,  $T_{\text{eff}}(2)$ , with the photometric effective temperatures is shown in Fig. 9. In this figure, most points lie close to the line of unit slope and zero intercept, although the scatter is larger than in Fig. 8. The mean difference for  $T_{\text{eff}}(B-V) >$

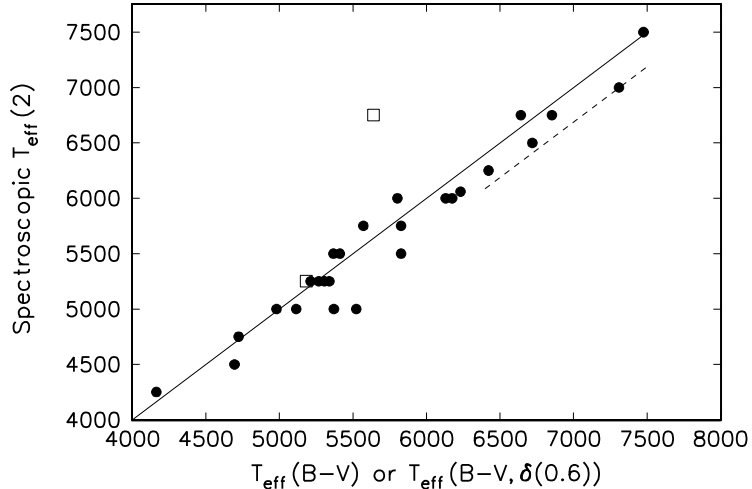


Figure 9: The spectroscopic effective temperature  $T_{\text{eff}}(2)$  plotted as a function of  $T_{\text{eff}}(B-V)$  for Population I stars (circles), and  $T_{\text{eff}}(B-V, \delta(0.6))$  for the subdwarfs (open squares). The lines are from Fig. 8. The discrepant open square is HIP 99267.

6400 K is equal to  $-112 \pm 64$  K. This value differs from zero by less than  $2\sigma$  suggesting that  $T_{\text{eff}}(2)$  does not suffer from the problem of underestimating effective temperatures of the hottest stars. The overall mean difference  $T_{\text{eff}}(2) - T_{\text{eff}}(B-V)$  is equal to  $-82 \pm 35$  K. Thus, the  $T_{\text{eff}}(2)$  scale is slightly cooler from the  $T_{\text{eff}}(B-V)$  scale.

## 5. The Photometric Surface Gravities

Using the  $uvby\beta$  indices from Table 2 (with the duplicity corrections for the binaries taken into account) and the program UVBYBETA, we have obtained the photometric surface gravities listed in Table 6. We have denoted these values by  $\log g(c_1, \beta)$  to indicate their sensitivity to  $c_1$  and  $\beta$ . No reddening corrections were applied. Because of the sensitivity to  $\beta$ , HIP 97168 was omitted; HIP 99267 was omitted because the program is not calibrated for subdwarfs.

A comparison of the spectroscopic  $\log g$  with  $\log g(c_1, \beta)$  is shown in Fig. 10. Filled circles have the ordinates obtained with the ELODIE grid (see Paper I, Table 9), and open squares, those obtained with the FRESCO grid (Paper I, Table 10). Deviant points are labeled with HIP numbers. The overall agreement between the spectroscopic  $\log g$  and  $\log g(c_1, \beta)$  is unsatisfactory in both cases.

## 6. Summary

We find no evidence that the program stars are reddened. In this we disagree with KIC-10 which gives  $E(B-V)$  ranging from 0.01 to 0.06 mag for nine of our program stars. Unfortunately, a detailed star-by-star comparison must be postponed until the catalog is made public.

The photometric effective temperatures derived in Sect. 4.1 from  $B-V$ ,  $T_{\text{eff}}(B-V)$ , agree very well with the spectroscopic effective temperatures given in Table 9 of Paper I, for  $T_{\text{eff}}(B-V) < 6250$  K. For  $T_{\text{eff}}(B-V) > 6400$  K, these spectroscopic effective temperatures, referred to in the present paper as  $T_{\text{eff}}(1E)$ ,

T a b l e 6  
The photometric surface gravities

HIP	$\log g(c_1, \beta)$	s.e.
PATS		
93011	4.27	0.10
94335	4.62	0.06
94565	4.02	0.16
94734	3.89	0.11
95098	3.96	0.20
95637	4.41	0.04
97974	4.74	0.07
The remaining program stars		
94145	4.16	0.06
94743	4.45	0.05
95843	3.94	0.12
96146	4.20	0.13

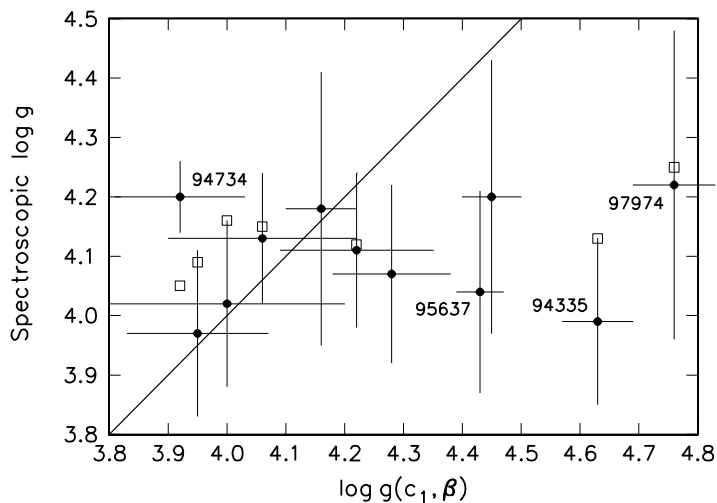


Figure 10: The spectroscopic  $\log g$  plotted as a function of the photometric  $\log g(c_1, \beta)$ . Filled circles have the ordinates obtained with the ELODIE grid, and open squares, those obtained with the FRESCO grid. The solid line has unit slope and zero intercept. Deviant points are labeled with HIP numbers.

are systematically smaller from the  $T_{\text{eff}}(B - V)$  by  $311 \pm 34$  K (see Fig. 8). The photometric effective temperatures  $T_{\text{eff}}(\beta)$ , derived in Sect. 4.1 from  $\beta$ , show very nearly the same problem: for  $T_{\text{eff}}(B - V) > 6400$  K, the difference  $T_{\text{eff}}(1E) - T_{\text{eff}}(\beta)$  amounts to  $-346 \pm 91$  K. Clearly, the calibrations of the  $T_{\text{eff}}(1E)$ ,  $T_{\text{eff}}(B - V)$  and  $T_{\text{eff}}(\beta)$  scales for F-type stars should be examined. We leave this as a task for the (near) future.

The photometric surface gravities of the program stars,  $\log g(c_1, \beta)$ , derived in Sect. 5 from  $c_1$  and  $\beta$ , range from  $3.89 \pm 0.11$  to  $4.74 \pm 0.07$ . The range of the spectroscopic  $\log g$  of Paper I is a factor of two smaller (see Fig. 10). Whether this is caused by incorrect spectroscopic  $\log g$  values of HIP 94734, HIP 94335 and HIP 97974 or by an error in the photometric surface gravities needs looking into.

## APPENDIX

### Photometric Reductions

For the *UVB* reductions we have used the following equations:

$$A_1 + B_1(B - V) + K_1X = C_{\text{BV}}^X + 0.03(B - V)X, \quad (1)$$

$$A_2 + B_2(U - B) + K_2X = C_{\text{UB}}^X, \quad (2)$$

and

$$A_3 + B_3(B - V) + K_3X = V^X - V, \quad (3)$$

where  $X$  is the air mass,  $C_{\text{BV}}^X$  is the raw blue-visual color index,  $C_{\text{UB}}^X$  is the raw ultraviolet-blue color index,  $V^X$  is the raw visual magnitude,  $A_1$ ,  $A_2$ ,  $A_3$  and  $B_1$ ,  $B_2$ ,  $B_3$  are the transformation coefficients, and  $K_1$ ,  $K_2$ ,  $K_3$  are the atmospheric extinction coefficients. In writing these equations we have assumed (1) the second-order extinction coefficient for the blue-visual color index to be equal to  $-0.03$ , (2) the second-order extinction coefficient for the ultraviolet-blue color index to be equal to zero, and (3) the second-order extinction coefficient for the visual magnitude to be equal to zero.

Each *UBV* observation of a standard star, consisting of  $X$ ,  $C_{\text{BV}}^X$ ,  $C_{\text{UB}}^X$  and  $V^X$ , was used to form three independent equations of condition, corresponding to Eqs. (1), (2) and (3). For a number of standard stars observed at a time, the equations of conditions were solved by the method of least squares using the standard color-indices and the standard magnitudes listed in columns 3, 4 and 2 of Table 7. Thus, Eqs. (1) yielded  $A_1$ ,  $B_1$  and  $K_1$ . These coefficients were then used to compute the  $B - V$  color-indices of program stars from  $C_{\text{BV}}^X$  and  $X$ ; because of the second term on the r.h.s of Eq. (1), this was done by iteration. In the next step,  $A_3$ ,  $B_3$  and  $K_3$ , which resulted from solving Eqs. (3), and the  $B - V$  just obtained were used to compute the  $V$  magnitudes of the program stars from  $V^X$  and  $X$ . The  $U - B$  indices of the program stars were computed from  $C_{\text{UB}}^X$  and  $X$  using  $A_2$ ,  $B_2$  and  $K_2$ . On most nights, observations of the standard stars were made before and after program stars' observations, so that the coefficients could be interpolated in order to compensate for their variation during the night.

In case of one standard star, HD 157881, the deviations from the solutions of Eqs. (1) were large but consistent, their mean value amounting to 0.046 mag. We concluded that the  $B - V$  index of this star given in reference (1) must be in error and adjusted it accordingly; the adjusted value is indicated in Table 7 with a colon.

In case of the *uvby* reductions, the equations for  $b - y$ ,  $m_1$  and  $y$  had the same form as the *UBV* equations just discussed, except that there was no need to include

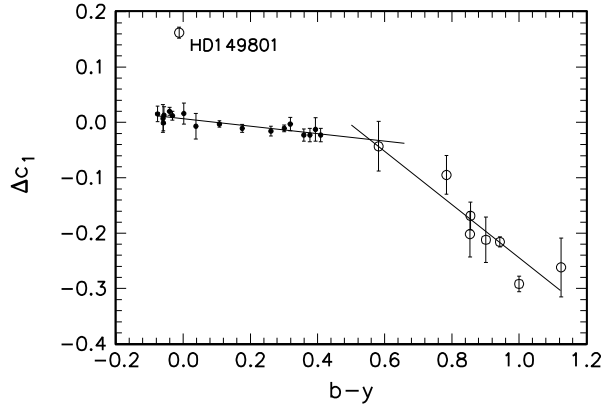


Figure 11: The  $c_1$  deviations for the standard stars (in the sense “computed *minus* standard”) plotted as a function of standard  $b - y$ . Filled circles are standard stars the  $c_1$  indices of which were used in solving Eqs. (7), while open circles are the remaining standard stars. The straight lines were fitted to the points by the method of least squares.

a second-order  $b - y$  extinction coefficient. Thus, the equations were the following:

$$a_1 + b_1(b - y) + k_1X = C_{by}^X, \quad (4)$$

$$a_2 + b_2m_1 + k_2X = C_m^X, \quad (5)$$

and

$$a_3 + b_3(b - y) + k_3X = y^X - V, \quad (6)$$

where  $X$  is the air mass,  $C_{by}^X$  is the raw  $b - y$  color index,  $C_m^X$  is the raw  $m_1$  index,  $y^X$  is the raw  $y$  magnitude,  $a_1$ ,  $a_2$ ,  $a_3$  and  $b_1$ ,  $b_2$ ,  $b_3$  are the transformation coefficients, and  $k_1$ ,  $k_2$ ,  $k_3$  are the atmospheric extinction coefficients.

Eqs. (4), (5) and (6) were solved using the raw color-indices and the raw  $y$  magnitudes of the standard stars and the standard values listed in Table 7. In case of  $m_1$ , HD 149801 and most standard stars redder than  $b - y = 0.5$  mag showed large deviations (of about  $\pm 0.05$  mag) from the solution, while the remaining standard stars showed deviations smaller than about  $\pm 0.01$  mag. Therefore, we solved Eqs. (5) again, using only the standard  $m_1$  values of these remaining standard stars. In Table 7, the  $m_1$  values not used in this final solution are indicated with a dollar sign.

The  $c_1$  reductions were began with solving the equations

$$a_4 + b_4c_1 + k_4X = C_1^X, \quad (7)$$

where  $C_1^X$  is the raw  $c_1$  index and the remaining symbols are analogous to those in the former equations, using all standard  $c_1$  values listed in column 8 of Table 7. However, the solution had an excessively large standard deviation. This was caused by the same standard stars that did not fit the  $m_1$  solution. Therefore, we rejected these standards and solved Eqs. (7) using standard  $c_1$  values of the remaining ones, indicated with an ampersand in column 8 of Table 7. The transformation coefficients  $a_4$  and  $b_4$ , and the extinction coefficient  $k_4$  obtained in this way yielded the deviations plotted as a function of  $b - y$  in Fig. 11.

As can be seen from Fig. 11, the deviations can be represented by two straight lines, a less inclined one for  $b - y < 0.6$  mag, and a more inclined one to the red

of  $b - y = 0.6$  mag. Taking this into account, we reduced the  $c_1$  observations of program stars in two steps. First, we computed intermediate values of  $c_1$  using Eq. (7) and the extinction and transformation coefficients obtained from the solution with the limited number of standards, and then, we corrected these intermediate  $c_1$  indices using the slopes and zero-intersect values of the lines shown in Fig. 11.

Finally, in the  $\beta$  reductions we have used the equation

$$a_5 + b_5\beta = \beta', \quad (8)$$

where  $\beta$  are the standard values from column 9 of Table 7 and  $\beta'$  are the raw values.

**Acknowledgments.** This work was partly supported by MNI<sub>SW</sub> grant N203 014 31/2650 and the University of Wrocław grant N<sub>Q</sub> 2646/W/IA/06. JM-Ż thanks the Danish Natural Science Research Council, the Italian National Institute for Astrophysics (INAF), and the University of Catania for financial support.

## REFERENCES

- Boesgaard, A.M., and Friel, E.D. 1990 *Astrophys. J.* 351 467  
Cameron, L.M. 1985 *Astron. Astrophys.* 146 59  
Carney, B.W., Latham, D.W., Laird, J.B., and Aguilar, L.A. 1994 *Astron. J.* 107 2240  
Crawford, D.L. 1975a *Astron. J.* 80 955  
Crawford, D.L. 1975b *PASP* 87 481  
Crawford, D.L. 1979 *Astron. J.* 84 1858  
Crawford, D.L., and Perry, C.L. 1976 *PASP* 88 454  
ESA 1997 “The Hipparcos and Tycho Catalogues” ESA SP-1200  
Flower, P.J. 1996 *Astrophys. J.* 469 355  
Hauck, B., and Mermilliod, M. 1998 *Astron. Astrophys. Suppl. Ser.* 129 431  
Johnson, H.L. 1966 *Ann. Rev. Astron. Astrophys.* 4 193  
Johnson, H.L., and Knuckles, C.F. 1955 *Astrophys. J.* 122 209  
Karataş, Y., and Schuster, W.J. 2006 *MNRAS* 371 1793  
Lang, K.R. 1992 *Astrophysical Data* Springer  
Mendoza, E.E. 1967 *Bol. Obs. Tonantzintla Tacubaya* 4 149  
Mermilliod, J.-C. 1991 *Catalogue of Homogeneous Means in the UBV System Institut d’Astronomie, Universite de Lausanne*  
Molenda-Żakowicz, J., Frasca, A., Latham, D.W., and Jerzykiewicz, M. 2007 *Acta Astron.* 57 301 Paper I  
Moon, T.T., and Dworetsky, M.M. 1985 *MNRAS* 217 305  
Oja, T. 1991 *Astron. Astrophys. Suppl. Ser.* 89 415  
Olsen, E.H. 1988 *Astron. Astrophys.* 189 173  
Olsen, E.H. 1993 *Astron. Astrophys. Suppl. Ser.* 102 89  
Olson, E.C. 1974 *Astron. J.* 79 1424  
Pinsonneault, M.H., Terndrup, D.M., Hanson, R.B., and Stauffer, J.R. 2004 *Astrophys. J.* 600 946  
Popper, D.M., Lacy, C.H., Frueh, M.L., and Turner, A.E. 1986 *Astron. J.* 91 383  
Prugniel, Ph., and Soubiran, C. 2001 *Astron. Astrophys.* 369 1048  
Sandage, A. 1969 *Astrophys. J.* 158 1115  
Sandage, A., and Eggen, O.J. 1959 *MNRAS* 119 278  
Spite, M., Francois, P., Nissen, P.E., and Spite, F. 1996 *Astron. Astrophys.* 307 172  
Taylor, B.J. 1980 *Astron. J.* 85 242  
van Leeuwen, F. 2007 *Astron. Astrophys.* 474 653

T a b l e 7  
Adopted standard magnitudes and color indices

HD	$V$	$B - V$	$U - B$	Ref.	$b - y$	$m_1$	$c_1$	$\beta$	Ref.
142860	3.845*	0.478	-0.025	(1)	0.319	0.150	0.401&	2.633	(3)
144206	4.738	-0.101	-0.321	(1)	-0.032	0.105	0.756&	2.756	(3)
146470	8.430	1.350	1.510	(1)	0.854	0.561\$	0.482	—	(3)
149801	—	—	—		-0.014	0.141\$	0.902	—	(3)
151288	8.102	1.369	1.289	(1)	0.784	0.757\$	0.030	2.508	(3)
154029	5.268	0.023	0.027	(1)	0.001	0.172	1.102&	2.885	(3)
157214	5.393	0.619	0.069	(1)	0.404	0.179	0.312&	2.590	(3)
157881	7.543*	1.314:	1.260	(1)	—	—	—	—	
158148	5.525	-0.135	-0.580	(1)	-0.040	0.091	0.435&	2.688	(3)
160346	6.533*	0.954	0.778	(1)	—	—	—	—	
160365	6.116*	0.556	—	(1)	0.374	0.162	0.555&	2.634	(3)
164058	2.242*	1.517	1.882	(2)	0.941	0.811\$	0.373	—	(3)
165401	6.806#	—	—	(1)	0.393	0.166	0.288&	2.580	(3)
176486	7.257#	—	—	(3)	1.125	0.735\$	0.310	—	(3)
178233	5.531	0.290	0.040	(1)	0.176	0.190	0.747&	2.758	(3)
184171	4.739	-0.142	-0.658	(1)	-0.057	0.095	0.376&	2.656	(3)
185395	4.475	0.382	-0.029	(1)	0.261	0.157	0.502&	2.688	(3)
186429	7.552#	—	—	(3)	0.855	0.607\$	0.496	—	(3)
188665	5.140	-0.136	-0.550	(1)	-0.059	0.098	0.453&	2.715	(3)
190993	5.068	-0.177	-0.692	(1)	-0.076	0.100	0.296&	2.686	(3)
195943	5.381	0.079	0.046	(1)	0.023	0.205	0.980&	2.920	(3)
196035	6.470	-0.140	-0.670	(1)	-0.060	0.087	0.287&	2.688	(3)
196090	7.787	1.412	1.560	(1)	0.901	0.596\$	0.444	—	(4)
198639	5.061	0.198	0.123	(1)	0.108	0.208	0.897&	2.843	(3)
201891	7.371	0.511	-0.158	(1)	0.358	0.104	0.262&	2.590	(3)
202575	7.950	1.044	0.840	(1)	0.581	0.568\$	0.205	—	(3)
207978	5.532	0.413	-0.125	(1)	0.299	0.122	0.425&	2.640	(3)
216397	4.983	1.559	1.926	(1)	1.000	0.750\$	0.450	—	(5)

\* Not used in the  $y$  reductions.

: Adjusted (see text).

# Used in the  $y$  reductions, but not in the  $V$  reductions.

\$ Not used in the final  $m_1$  reductions.

& Used in solving Eqs. (7).

(1) Mermilliod (1991).

(2) Oja (1991).

(3) Hauck & Mermilliod (1998).

(4) Olsen (1993).

(5) Olson (1974).